Computers and Geotechnics 101 (2018) 34–47

Contents lists available at ScienceDirect

Computers and Geotechnics

journal homepage: www.elsevier.com/locate/compgeo

Research Paper

Probabilistic stability analysis of an earth dam by Stochastic Finite Element Method based on field data

A. Mouyeaux[a,b], C. Carvajal[a,*], P. Bressolette[b,c], L. Peyras[a], P. Breul[b,c], C. Bacconnet[b,c]

[a] Irstea, UR RECOVER, 3275 Route de Cézanne, CS 40061, 13182 Aix-en-Provence Cedex 5, France
[b] Université Clermont-Auvergne, Institut Pascal, BP 10448, F-63000 Clermont-Ferrand, France
[c] CNRS, UMR 6602, Institut Pascal, F-63171 Aubière, France

ARTICLE INFO

Keywords:
Earthfill dam
Finite element method
Strength reduction method
Spatial variability
Slope stability
Reliability

ABSTRACT

This paper performs a probabilistic stability analysis for an existing earthfill dam using a Stochastic Finite Element Method (SFEM) and considering the spatial variability of soil properties based on field data. Previous works on probabilistic slope stability analysis are generally based on hypothetical data while using data from existing earth structures is not widespread.

A probabilistic procedure based on field data is here implemented to analyze the stability of an existing embankment dam. The spatial variability of several soil properties is modeled from the geostatistical analysis of the available dataset of the dam studied. Random variables and random fields representing the variability of dam materials are integrated into an FE model by performing Monte Carlo simulations (MCS). This probabilistic analysis based on field data allowed to characterize the variability of the sliding safety factor for the case study of an existing dam.

1. Introduction

The probabilistic analysis of slope stability is a topic that has been widely studied in the literature. Works in this domain have mainly considered uncertainties relating to soil mechanical properties obtained from geotechnical investigations. These uncertainties essentially stem from inherent spatial variability and measurement errors [1,2], to which can be added limited site investigation data and the assumptions included in the stability model [3]. Among these sources of uncertainties, some studies have shown that spatial variability is the most important [4–6]. Therefore, it is the aspect on which research studies have focused most [2,3,7–16]. Thus, the theory of random fields [17] is best suited for modeling the spatial variability of properties of continuous media like soils. In recent years, much research has integrated this kind of modeling in embankment slope stability analysis covering different aspects. For example, Gaouar et al. [18] and Auvinet and Gonzalez [19] studied the reliability of hypothetical earth dams using random fields of undrained shear strength. Nishimura et al. [47] employed the Swedish weight sounding test to identify the spatial correlation structure of the materials of an earth-fill dam. Zheng et al. [48] conducted a Bayesian updating approach with monitoring data to improve the predictions of embankment settlements. Cho [11] used direct MCS to investigate the effect of the spatial variability of shear strength parameters on the failure surface with 1-D random fields and LEM. Others have paid attention to the influence on both seepage and slope stability of the characteristics of random fields like: (i) correlation length [2,20]; (ii) the coefficient of variation (CoV) [14]; (iii) the choice of the autocorrelation function (ACF) used to represent spatial variability [3,16]. Finally, Liu et al. [3] proposed a numerical procedure to combine Subset Simulations (SS) with the Kriging method for assessing the reliability of an embankment slope in spatially variable soils.

Most of these studies used the limit equilibrium method (LEM) to assess slope stability. However, with the rapid development of computational tools, FEM is increasingly used in geotechnics. This is particularly true concerning sliding stability analyzes [21] which have been extensively combined with the strength reduction method (SRM), based on Zienkiewicz's work [22]. SRM has since been used for slope stability analyzes by many authors like Matsui and San [23], Griffiths and Lane [24], Cheng et al. [25], Huang and Jia [26] and others. Combined with SRM technique, FEM is used as an alternative to LEM because it presents several advantages that are described in detail in [24,25]: (i) no assumptions are needed concerning the failure surface, (ii) no assumptions on inter-slice side forces are needed, since there is no concept of slices, and (iii) soil behavior can be modeled in terms of

* Corresponding author at: Irstea, UR RECOVER, 3275 Route de Cézanne, CS 40061, 13182 Aix-en-Provence Cedex 5, France.
E-mail addresses: anthony.mouyeaux@irstea.fr (A. Mouyeaux), claudio.carvajal@irstea.fr (C. Carvajal), philippe.bressolette@uca.fr (P. Bressolette), laurent.peyras@irstea.fr (L. Peyras), pierre.breul@uca.fr (P. Breul), claude.bacconnet@uca.fr (C. Bacconnet).

https://doi.org/10.1016/j.compgeo.2018.04.017
Received 21 June 2017; Received in revised form 6 April 2018; Accepted 20 April 2018

stresses/strains. Furthermore, several studies have shown that LEM and SRM give similar FoS [24,25], except in some specific cases pointed out by Cheng et al. [25].

Different methods are used in the literature to evaluate reliability in geotechnical issues. Some authors used first-order, second-moment (FOSM) methods [2,7,27], whereas others used the FORM method [11,20,28]. MCS is nevertheless the method used most for probabilistic slope stability analysis [3,8,9,13,15,16]. MCS is a simple and robust tool for simulating the statistical distribution of FoS, although it requires considerable computational effort in terms of calculation time [13,15].

Regarding earthfill dams, large quantities of geotechnical data are available in the form of design studies, construction controls and monitoring measurements [29,30]. These data are still not well exploited in studies relating to the reliability of earth dams (or for that of concrete dams [33]), although some authors have underlined the benefits of carrying out a geostatistical analysis on them [31,32]. However, the probabilistic assessment of geotechnical properties generally depends on the type of soils and considerations found in the literature, such as in the work of Phoon and Kulhawy [5,6].

Thus, all the studies mentioned above concern one or several aspects of earth dam reliability. The lack of global studies involving all the aspects involved, and most particularly the use of real data through geostatistical approaches, is regrettable.

This article describes a probabilistic procedure, based on several elements available in the literature, to assess the reliability of an existing earth dam using the stochastic finite element method (SFEM). The originality of this work is to base probabilistic developments on the dataset available on the case study. The spatial variability of several properties of the embankment materials are modeled from these data with random fields. The uncertainties are then spread using MCS in a coupling between a mechanical FE model and a reliability model in order to simulate the statistical distribution of the FoS. The article implements a similar approach to the probabilistic modeling of the pore water pressure inside an earth dam [30].

This article is organized as follows: Section 2 presents the different theoretical notions already available in the literature and which are used in the probabilistic procedure. The case study and the available dataset are also described in this section. Section 3 presents the general principle of the probabilistic procedure implemented on the studied earth dam. This section also describes the development of the deterministic FE model and the probabilistic modeling based on the field data of the case study. Finally, the results obtained are discussed and the main conclusions are summarized in the last section.

2. The stochastic finite element method for sliding stability analysis

2.1. Factor of safety calculation by SRM in FEM

Slope stability analysis by FEM has been performed extensively using SRM. The general principle of SRM is to incrementally reduce the values of effective shear strength parameters until failure occurs. The initial shear strength parameters c' and $\tan\varphi'$ are reduced by a factor F to give the parameters c'_{red} and $\tan\varphi'_{red}$ used in the calculations:

$$c'_{red} = c'F \quad \varphi'_{red} = tan^{-1}(\tan\varphi'/F) \tag{1}$$

The FoS is considered as the factor of reduction F at failure. This leads to the same definition of the FoS as in LEM [21,24,26].

Most studies using SRM consider the Mohr-Coulomb (MC) failure criterion in the analyzes [13,24,26,34], above all due to its relative simplicity. This failure criterion presents the advantage of being directly dependent on the shear strength parameters c' and $\tan\varphi'$. However, this criterion can lead to computational difficulties caused by the irregularities of its hexagonal pyramidal yield surface. Some authors have proposed solutions to overcome this difficulty through using an approximate MC failure criterion [35]. In the case of study presented in this article, the Drucker-Prager (DP) criterion is chosen as an approximation of the MC criterion. The DP criterion is very close to the MC criterion, except that it has the advantage that the conical yield surface of the DP criterion allows better convergence of the calculations in the FE model. Furthermore, the DP criterion's parameters can be linked to the shear strength parameters, c' and $\tan\varphi'$, and to the dilatancy angle ψ', through simple relations described in the literature [36].

For SRM, the non-convergence of the FE model is generally taken as an indicator of failure occurrence, although other definitions are possible [24]. This definition of (numerical) failure has the advantage of simplicity of implementation but the disadvantage of not having a physical basis.

Slope stability analyzes involving saturated/unsaturated seepage could be performed through two approaches [26]. On the one hand, the seepage and stress/deformation calculations can be done independently. The results of hydraulic FE modeling, i.e. pore water pressures, matric suctions and saturation level are used as inputs in the mechanical FE model. The elasto-plastic calculations are thus performed in terms of effective stresses. On the other hand, the coupling between hydraulic and mechanical calculations can be stronger. In that case, the iterative procedure involves both seepage and deformation calculations which are performed at every step. This approach demands a massive computational effort and is used in specific cases that require considering the effects of consolidation. Thus, the first approach is more often preferred because of its relative simplicity and effectiveness [26].

Taking into account the configuration of the dam studied, an uncoupled approach was used for the seepage analysis in the case study. The present article will focus on the mechanical part, since that concerning seepage has already been presented in a previous work [30].

2.2. Spatial variability modeling

Soils used to build embankment dams are natural materials whose properties are by nature highly variable [11]. Spatial variability represents the main part of soil variability because of the combination of geological, environmental, physical and chemical processes [5]. Soils are heterogeneous in natural state but this heterogeneity is also present in human constructions like earth dams. Although embankment materials are rearranged beforehand and are subjected to continuous control during construction, the layer-based construction method does not eliminate this spatial variability.

To accommodate the spatial variations of soil properties, the random field theory has been widely used recently in the literature relating to geotechnical issues, and most particularly to slope stability [2,3,11–16,26,37,38,46]. A development of this theory can be found in [17]. Random fields can represent spatial variability but, if considered as Gaussian, they require the definition of at least the statistical moments, i.e. mean and standard deviation, and the autocorrelation function (ACF). These characteristics are generally estimated from hypothetical or statistical considerations. However, geostatistics allow analyzing and modeling a spatial phenomenon in interpreting the behavior of an existing sample [32]. The first step of a geostatistical analysis is to describe variability by a function of the structure $\gamma(\mathrm{h})$, called a variogram, which represents the semi-variance between the deviation of the values taken by a point at position $\mathrm{x_i}$ and a second separated from the first by distance h. In practice, preference is given to an estimator of the theoretical variogram, often called experimental variogram $\gamma^*(\mathrm{h})$, given by Eq. (2):

$$\gamma^*(\mathrm{h}) = \frac{1}{2\mathrm{N(h)}} \sum_{\mathrm{i=1}}^{\mathrm{N(h)}} [\mathrm{Z(x_i + h) - Z(x_i)}]^2 \tag{2}$$

where N(h) is the number of pairs of variable Z(x) separated by distance h.

If the sample is not regularly spaced, the sampled pairs are regrouped into intervals in which the average distance is used instead of h [32]. Then, a mathematical model is applied to the experimental variogram and permits representing either the theoretical variogram directly, or the ACF, which will allow the generation of the random fields [17]. The exponential model, described by Eq. (3), is one of the most common variogram models used as ACF in the literature.

$$\gamma(\mathrm{h}) = \mathrm{C}[1-\mathrm{e}^{-(\delta \mathrm{h}/\mathrm{a})}] \quad \delta = 2.996 \tag{3}$$

The parameter C is the sill value at which the variogram levels off. This value represents the order of magnitude of the variability along the considered axis and it is homogenous to the variance value of the overall data. The parameter a represents the range of the variogram (also called autocorrelation distance). It is the distance at which the variogram reaches the sill value: there is no correlation beyond this distance. For bounded models like the exponential model, the sill is reached asymptotically and the autocorrelation distance (also called the practical range) is equal to the scale factor a/δ corresponding to the distance where the variogram reaches 95% of the sill.

In this article, stationary Gaussian random fields with an exponential ACF are taken into account for their simplicity, and for consistency with most of the studies on the subject. Further developments could be accomplished to extend the approach proposed to more complex random fields (i.e. non-Gaussian or non-stationary random fields) but they are beyond the scope of this article.

2.3. Reliability approach

The deterministic value of the FoS is generally not sufficient for evaluating the global safety of the slope of an embankment [39], in particular in a risk analysis. In recent years, reliability approaches have been developed and used in the domain of slope stability analysis [4,11,13,27,39–41,46]. The reliability approach is based on the definition of a performance function $g(\boldsymbol{X})$ in which $\boldsymbol{X}$ represents a random vector of the input variables. This function defines the limit state surface separating the safe and unsafe regions. It can be described mathematically as: $g(\boldsymbol{X}) = 0$ on the limit state surface, $g(\boldsymbol{X}) > 0$ on the safety domain, and $g(\boldsymbol{X}) < 0$ on the failure domain [27]. Regarding the slope stability problem, the performance function is usually used in the form defined by Eq. (4).

$$g(\boldsymbol{X}) = FoS-1 \tag{4}$$

The performance function $g(\boldsymbol{X})$ is evaluated in our case through the numerical FE model. A major advantage of the reliability approach is that it permits evaluating the variability of output variables of the performance function $g(\boldsymbol{X})$, which then yields other results such as the probability of failure P_f and the reliability index β. Thus, this article will focus on the variability of the FoS (obtained by the FEM) by evaluating the mean and standard deviation. The failure probability is linked to the performance function and is defined as:

$$\mathrm{P}_f = P[g(\boldsymbol{X}) < 0] = \int_{g(\boldsymbol{X}) < 0} f_X(\boldsymbol{X}) d\boldsymbol{X} \tag{5}$$

where $f_X(\boldsymbol{X})$ is the joint probability density function of the input variables [13]. This integral is however too difficult to evaluate directly because it is practically impossible to know the joint probability density function $f_X(\boldsymbol{X})$ and the integration domain exactly.

Different methods exist to overcome this difficulty. In the field of slope stability, one of the most commonly used methods is to evaluate the uncertainties through a reliability index β. There are many definitions of reliability index [39]. Most of them involve the first two statistical moments of the FoS distribution, i.e. mean μ_{FoS} and standard deviation σ_{FoS}. In the present article, the reliability index used is given by Eq. (6), following a form used in several studies [4,27,39–41].

$$\beta = \frac{\mu_{FoS}-1}{\sigma_{FoS}} \tag{6}$$

In the approach adopted, MCS are first used to evaluate the variability of FoS and then as an alternative to evaluate the integral of Eq. (5) [11]. Indeed, this method allows computing the distribution of the performance function in generating the values of the different random input variables according to their specific probability distributions. This approach requires repeating the procedure many times in order to obtain a robust response of the FE model. The computational effort needed is offset by the relative simplicity of the MCS.

2.4. Dam studied and available data

The earth dam analyzed is a pseudo-zoned dam located in France. It is a 23 m high and 170 m long structure which closes a valley covered with alluvial deposits. The dam body includes three zones: a core (COR) composed of sandy silts and two shoulders (UPS: upstream shoulder and DOS: downstream shoulder) made of coarse sands. Both materials are relatively similar (pseudo-zoned dam) and they stem from the alteration of schists composing the bedrock. The downstream shoulder is composed of a material slightly coarser than that of the upstream shoulder. The foundation is also composed of more or less altered schists whose superficial layers have been purged. The main cross-section of the structure is shown in Fig. 1.

Different data are available on the earth dam studied. These data are divided into two categories according to their origin along the dam lifecycle: preliminary studies or construction (test board or compaction controls). Table 1 presents an overview of the data available for the case study.

Regarding the data stemming from preliminary studies, about thirty samples had been taken from borrow pits for both materials composing the structure. These samples were subjected to grain size distribution

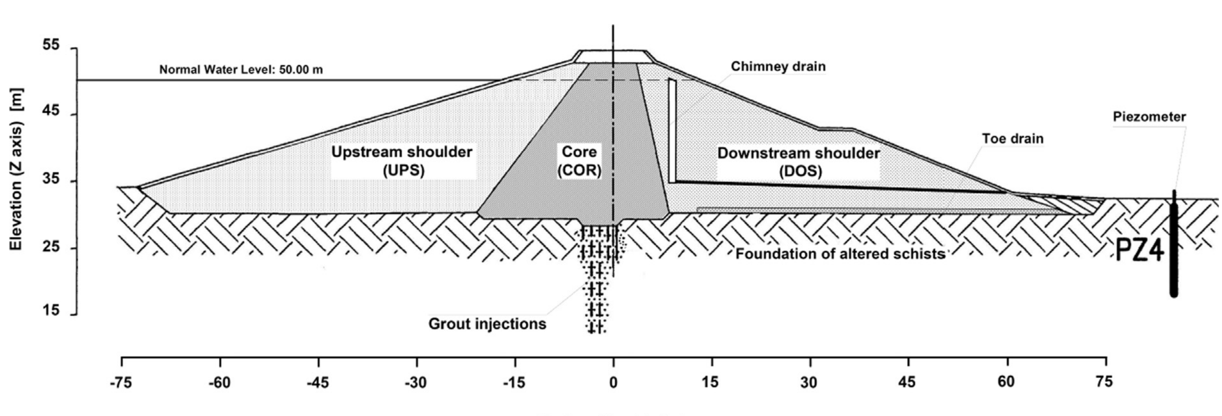

Fig. 1. Standard cross-section of the dam studied.

Table 1
Overview of the data available.

Soil type*	Samples		Grain-size distribution		Atterberg limits		CU triaxial tests		UU triaxial tests		Oedometer tests		Compaction tests		Dry density		Water content	
	(1)	(2)	(1)	(2)	(1)	(2)	(1)	(2)	(1)	(2)	(1)	(2)	(1)	(2)	(1)	(2)	(1)	(2)
Preliminary studies	11	13	10	13	3	12	5	3	2	2	2	2	5	5	0	0	0	0
Construction (test board)	11	0	11	0	0	0	0	0	0	0	0	0	0	0	0	0	0	0
Construction (compaction controls)	16	14	16	14	0	0	0	0	0	0	0	0	10	14	376/333	419	376/333	419
Total	38	27	37	27	3	12	5	3	2	2	2	2	12	19	376/333	419	376/333	419

* (1) UPS/DOS: Coarse sands (shoulders material); (2) COR: Sandy silt (core material).

analyzes, and other laboratory tests including identification tests (Atterberg limit measurements) and mechanical tests (triaxial tests, compaction tests and oedometer tests) were performed on some of them. However, Table 1 shows that only a few of these mechanical tests were available. The triaxial test results are presented in Table 2. They show that the two materials (i.e. sandy silts of the core and coarse sands of the shoulders) have roughly similar long-term behaviors with similar values for both the effective friction angle φ' and effective cohesion c'. Nonetheless, the two materials differ concerning the undrained shear strength characteristics with less friction and better undrained cohesion for the finer materials constituting the core.

Afterwards, a test section was delimited to evaluate the compaction of the materials through grain size distribution analyzes and plate bearing tests. Then, compaction controls were performed during the construction of the dam. These controls essentially consisted of water content and dry density measurements determined in-situ with a gamma-densimeter. In all, more than a thousand measurements were performed in the three zones (UPS: 376, COR: 419, DOS: 333, respectively), most of which have been geolocated (Fig. 2). The control measures were compared to the results of Proctor tests performed periodically during construction on samples taken directly from the three zones of the earth dam under construction. About twenty grain size distribution analyzes performed on the same samples completed the dataset.

The quantity of available data on the dam studied corresponds to the typical dataset of an earth dam of the same dimensions. In addition, the case study has the advantage that a reference system was installed during its construction, which made it possible to localize the compaction control measurements in space (according to the three axes). This system consists of a grid formed by ten profiles (P0 to P9) in the longitudinal direction (Y axis) and thirteen profiles (A to M) in the transversal direction (X axis) (see Fig. 2). The longitudinal profiles are 20 m spaced along the Y axis, excepted between P8 and P9 where the space is equal to 10 m. The transversal profiles are 13 m spaced along the X axis from profiles A to E and I to M, and 8 m spaced from profiles E to I. The compaction control measures (dry density and water content) were generally performed on the grid, but not systematically, as seen on Fig. 2. The grid permits the localization of the measurements on the (X-Y) plan and the knowledge of the construction layer gives the elevation of the measurements along the Z axis. Therefore, among the set of available dry density measurements, a large number of these measurements have a relatively precise localization in the space (UPS: 248, COR: 381, DOS: 272, respectively). Therefore, among the set of available dry density measurements, a large number of these measurements have a relatively precise localization in the space (UPS: 248, COR: 381, DOS: 272, respectively). Fig. 2 shows three plan views of the compaction control locations.

3. Probabilistic stability analysis of the case study

3.1. Steps of the probabilistic FoS modeling

This section presents an overview of the procedure implemented on the case study in order to evaluate the statistical distribution of the FoS based on the available data measured on the dam materials. The procedure adopted follows the steps described hereinafter.

(1) collect the available data on the dam under study;
(2) choose an elasto-plastic criterion to model the mechanical behavior of the dam materials. In this case, the DP criterion is chosen as an approximation of the MC criterion, under a formulation allowing to model the dilatancy and the hardening;
(3) determine from the available data the deterministic values of the material properties that participate in the safety evaluation model (seepage analysis and elasto-plastic criterion). This determination is achieved by using transformation models between the direct measurement from the geotechnical tests and design parameters. Reviews of such models were proposed by Kulhawy and Mayne

Table 2
Triaxial tests available on the dam studied.

	Coarse sands (UPS&DOS)					Sandy silts (COR)		
Samples	M01	F05	F09	F14	F14_bis	E50	F28	F29
% passing 80 µm	10%	6%	5.5%	8%		56%	43%	55%
% passing 2 µm	–	3%	2%	2.5%		23%	16%	19%
CU + u triaxial tests								
Effective friction angle φ'	33°	34°	35°	33°	36°	32°	36°	35°
Effective cohesion c'	15 kPa	8 kPa	0 kPa	10 kPa	14 kPa	15 kPa	5 kPa	10 kPa
UU triaxial tests								
Undrained friction angle φ_{UU}	15°			16°		0°	0°	
Undrained cohesion C_{UU}	70 kPa			49 kPa		125 kPa	126 kPa	

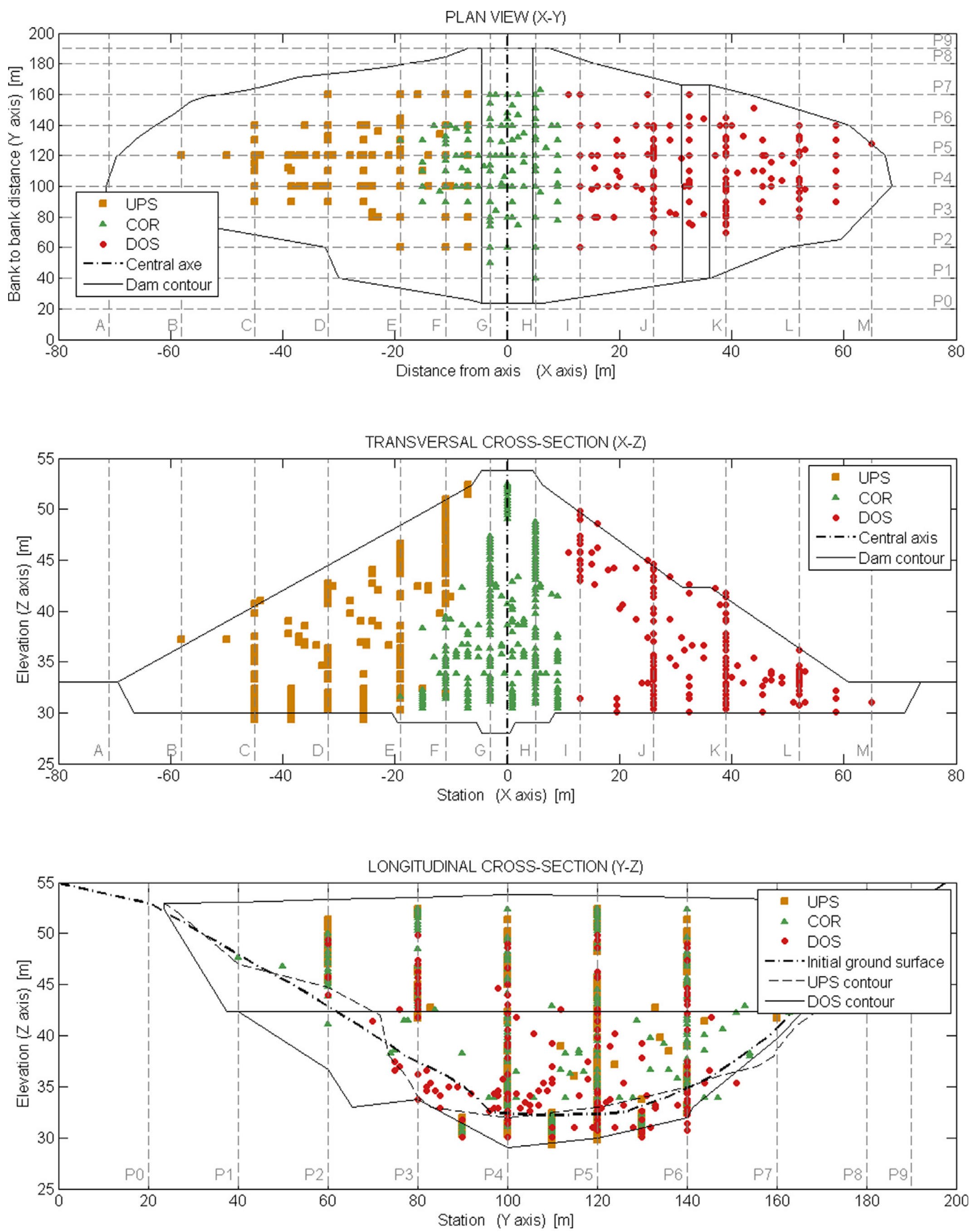

Fig. 2. Locations of compaction control in the dam studied.

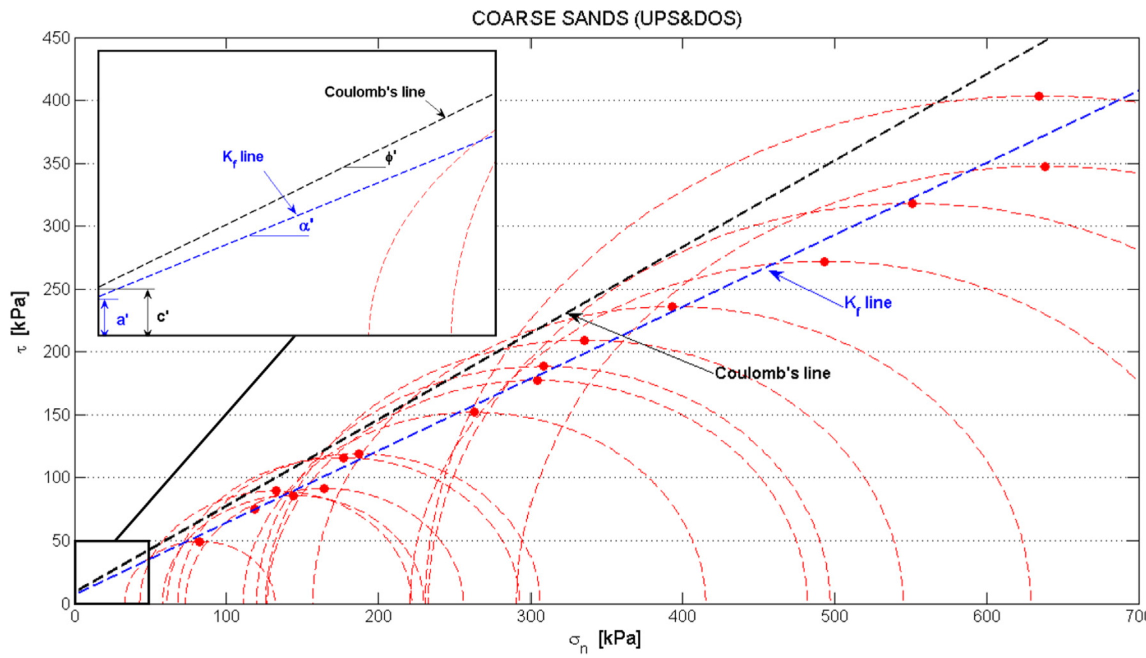

Fig. 3. Regression on Mohr's circles from available CU triaxial tests.

[42] and Monnet [43]. These two reviews include theoretical or empirical relationships linking in-situ or laboratory measurements to geotechnical parameters involved in the mechanical behavior of the soil. In this case study, the friction angle φ is related to the void ratio e (and so indirectly to the dry density) by Caquot's relationship described by Eq. (7), where k represents a constant:

$$e\cdot\tan(\varphi) = k \tag{7}$$

(4) construct a deterministic FE model in order to evaluate the slope stability of the structure. This model enables the calculation of the FoS with the SRM. For this case study, an open-ended FE code was chosen to add specific developments inherent to the approach, such as random field generation;
(5) perform a sensitivity analysis of the parameters to identify those which have a significant influence on the FoS and have to be modeled probabilistically. According to Griffiths and Lane [24], among the six mechanical parameters required for accurately modeling elasto-plastic behavior (i.e. friction angle, cohesion, dry density, Young's modulus, Poisson's coefficient and dilatancy angle) the first three have a significant influence on the FoS;
(6) give a probabilistic description of the parameters of interest emphasized in step (5). At this stage, the parameters can be represented as random variables thanks to a statistical analysis of the available data and the transformation models used in step (3);
(7) perform a geostatistical analysis of the compaction controls measurements (dry density). As there are sufficient and localized data, this analysis will give horizontal and vertical experimental variograms. These variograms give information on the spatial variability of the dry density which can be then modeled as a random field;
(8) use previous statistical and geostatistical analysis to obtain a spatial representation of all the influential parameters. The aim here is to model the spatial variability of every important parameter with random fields using transformation models and the random field of dry density from step (7);
(9) perform probabilistic analysis in running MCS from the deterministic FEM model developed in step (4). Numerous runs are necessary to characterize the variability of the FoS. The number of runs to be performed must be sufficient to obtain the convergence of the statistical moments (i.e. mean and standard deviation) of the FoS.

3.2. Deterministic FE model for slope stability

The case study dam was modeled with the Cast3M FE code. This code was not initially developed to treat geotechnical issues. However, the Cast3M code is an open-source code that allows the integration of user-developed procedures, which is highly beneficial for probabilistic analysis. The next subsections present the procedures developed in this study. For the sake of simplicity, only the situation corresponding to the normal operating level with a constant reservoir level is considered in the following. Other research works propose to model the reservoir level by a random variable based on hydrological considerations [44]. The mechanical behavior on which this study focuses is therefore long-term behavior with effective shear strength parameters.

3.2.1. Soil elasto-plastic behavior and deterministic values of the parameters

As seen in Section 2.1, the FE model developed considers the DP criterion as an approximation of the MC criterion. The input parameters of the DP criterion (α, β and κ) are expressed from the MC criterion parameters (friction angle φ', cohesion c' and dilatancy angle ψ') using the available relationships [36]. The aim is to give a deterministic value from the available data to the input parameters (φ', c' and ψ'), as well as those needed to simulate the loads acting on the dam: pore water pressures, self-weight and hydrostatic pressure. The probabilistic modeling of the spatial variability of pore water pressures was dealt with in a previous study [30] and only the mechanical parameters will be treated here. Finally, seven parameters had to be considered: dry unit weight γ_d, friction angle φ', cohesion c', dilatancy angle ψ', a hardening parameter H and elasticity parameters, i.e. E' and ν'.

Concerning dry unit weight, the deterministic values adopted corresponded to the mean of the measurements mentioned in the previous section, with values of 19.8 kN m^{-3} and 17.9 kN m^{-3} for coarse sands and sandy silts, respectively.

Concerning the shear strength parameters, only a small number of triaxial tests were available. In order to optimize these tests, the following process was adopted: (i) all the Mohr's circles linked to all the CU triaxial tests are reported on a single graph; (ii) the linear regression is determined on the top of the circles (K_f line); (iii) this line is transposed into the Coulomb line thanks to the relationships $\sin\varphi' = \tan\alpha'$ and $c' = a'/\cos\varphi'$, where α' and a' are parameters defining the K_f-line (see Fig. 3). The values obtained are given in Table 3. The dilatancy angle is then obtained from the friction angle in the empirical

Table 3
Mean value of input parameters.

Properties	Mean value	
	Coarse sands (UPS&DOS)	Sandy silts (COR)
Dry unit weight γ_d (kN m^{-3})	19.8	17.9
Friction angle φ' (°)	34.8	34.1
Cohesion c' (kPa)	8.9	13.4
Dilatancy angle ψ' (°)	12	12
Hardening H	100	100
Elastic modulus E' (MPa)	45	40
Poisson's ratio ν'	0.33	0.33

relationships described in [42,43]. Given the similarity between the values of the friction angle for the two materials, dilatancy angles close to 12° are computed for both materials.

The CU triaxial tests are also used to determine the deterministic values of the elastic modulus and the hardening parameter. These values correspond to the mean slopes of the two parts of the deviatoric stress vs. strain curves. Finally, Poisson's ratio is taken as equal to 0.33 because there is no data to determine its value from the available measurements. Table 3 synthetizes the deterministic values adopted for all the input parameters.

3.2.2. Validation of the FoS calculation

A 2D model is generally adopted in engineering as well as in the scientific literature to analyze the sliding mechanism [2–4,11–15,18,20,24–28,34,37]. Thus, for the FE model developed in this work, a 2D model was adopted in order to facilitate the analysis of the studied dam (in particular for the validation of the FoS calculation). Nonetheless, the subsequent development of a 3D model can also be of interest [19,46] given the geometry of the studied dam (having a length and a width of the same order of magnitude).

In the FE model developed, SRM was implemented by a user-specific procedure in the Cast3M code. This iterative procedure reduces the strength parameters from initial deterministic values and searches a new equilibrium state with reduced parameters starting from an initial stress field. The FoS is obtained with an interpolation technique of the maximal displacement vs. the factor of reduction F curve. By fitting a vertically asymptotic equation to this curve, the FoS can be predicted more accurately as the parameter reduction is implemented. This technique allows avoiding a non-convergence which would cause the FE code to stop (which could be very detrimental to MCS).

The commercial software SLOPE/W using LEM (Spencer method with search for circular slip surfaces) is here used to validate the FE model developed with the Cast3M code. LEM and FEM models using a similar hypothesis are compared to the deterministic case in Fig. 4. The FoS values computed (SLOPE/W: 2.71; Cast3M: 2.64) are close but not equal as is the location on the failure surface. Fig. 5 presents a direct comparison of the FoS computed with the two models for ten different parameter sets obtained randomly. The results are close to the unit line which validates the FoS obtained by the FE model developed.

3.2.3. Sensitivity analysis

A deterministic sensitivity analysis was performed on the parameters mentioned on last subsection on ranges of values corresponding to the measurements performed on the materials composing the dam studied. The sensitivity analysis results are synthetized in Fig. 6. The crosses represent the minimal and maximal values of the FoS obtained for each parameter for the variation ranges specified in the figure.

Afterwards, the influence of three mechanical properties is drawn: dry unit weight γ_d, friction angle φ', cohesion c'. These properties are considered probabilistically while the others will be considered with their deterministic values listed in Table 3. In Fig. 6, the arrows represent the FoS variation obtained for the dry unit weight, cohesion and friction angle parameters using the mean ± standard deviation values (showed in Table 4).

3.3. Probabilistic analysis with spatial variability modeling

3.3.1. Probabilistic assessment of parameters of interest

Modeling the three parameters – dry unit weight γ_d, friction angle φ' and cohesion c' – as random variables from available data is done by considering the previous steps. First, regarding dry unit weight γ_d, a statistical analysis of the compaction control sample measurements is performed. For both materials, the dry unit weight distribution can be represented by a normal distribution (χ^2 test). Truncated distributions are used in order to avoid unrealistic values. The mean of these distributions corresponds to the one listed in Table 3, whereas the bounds correspond to the extreme values really measured in the field.

For the shear strength parameters – i.e. friction angle φ' and cohesion c' – random variables can be determined with the regressions performed on the Mohr's circles obtained from the CU triaxial tests (Fig. 3). The distributions of the shear strength parameters were obtained by MC simulations, by propagation of the uncertainties of the intermediate parameters a′ and α′ (evaluated by linear regression to obtain the Kf line). The linear regression performed on the top of the Mohr circles to determine the Kf line gives the mean and the standard deviation of the two regression parameters (a′ and α′). By adopting a normal distribution, a sample of one million values was generated randomly for each of the regression parameters a′ and α′. A value of c' and φ' is then calculated for each pair of a′ and α′ thanks to the relationships $\sin\varphi' = \tan\alpha'$ and $c' = a'/\cos\varphi'$. These Monte Carlo simulations lead to generating a million values for the shear resistance parameters c' and φ', allowing thus to evaluate their dispersion (standard deviation or CoV). Thus, Monte-Carlo simulations make it possible to propagate the uncertainties of the regression parameters on the evaluation of the shear strength parameters (but they will not increase the information on the variability of shear strength parameters). Therefore, the resulting distribution represents the uncertainty of the evaluation of shear strength parameters from a small sample of available measurements. During simulations, the distributions of the shear strength parameters have been truncated to avoid unrealistic values. Given the small number of triaxial tests available, a wider truncation interval was adopted than observed from these tests.

The characteristics of the random variable distributions are described in Table 4.

3.3.2. Geostatistical analysis of compaction control measurements

At this stage, the parameters of interest for the sliding study – i.e. dry unit weight γ_d, friction angle φ' and cohesion c' – can be modeled as random variables from the available data. Nonetheless, their spatial variability could be taken into account by performing a geostatistical analysis of the available geolocalized data. This analysis is therefore performed on the numerous dry density measurements carried out in-situ for compaction control of the whole dam. Eq. (2) is used to assess the experimental variograms on each of the three zones of the dam (UPS, COR and DOS) in the vertical and horizontal directions. The horizontal direction corresponds to the upstream/downstream direction for stability analyzes performed in 2D. The autocorrelation lengths are obtained by fitting an exponential model on these experimental variograms (see Section 2.2). Fig. 7 shows the experimental variograms calculated for the downstream shoulder (DOS) in the horizontal and vertical directions (dashed broken lines), as well as the exponential variograms fitted to them (solid lines). The black squares on the exponential variograms in Fig. 7 represent the points in where 95% of the total variance is reached. The abscissa of these squares is considered as the autocorrelation distances (practical range), respectively in the horizontal direction (l_x = 4.9 m) for the left plot and in the vertical direction (l_z = 1.9 m) for the right plot.

Table 5 details the results obtained from the geostatistical analysis. Knowing these autocorrelation lengths and the two first statistical moments (i.e. mean and standard deviation) makes it possible to

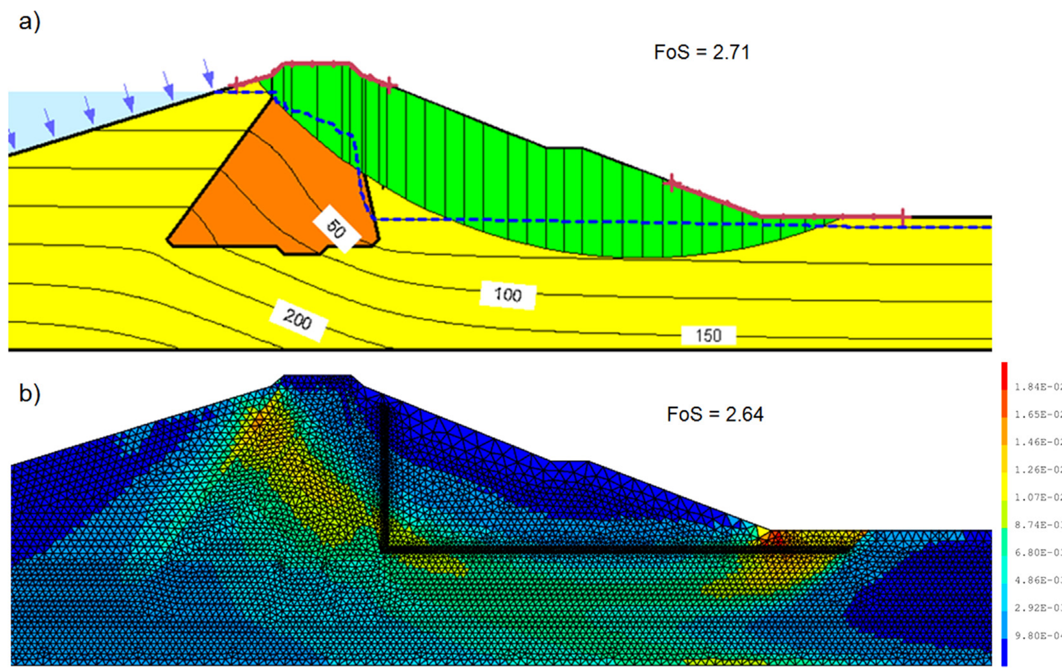

Fig. 4. Comparison of LEM and FEM: (a) SLOPE/W, (b) Cast3M (maximal shear strain field).

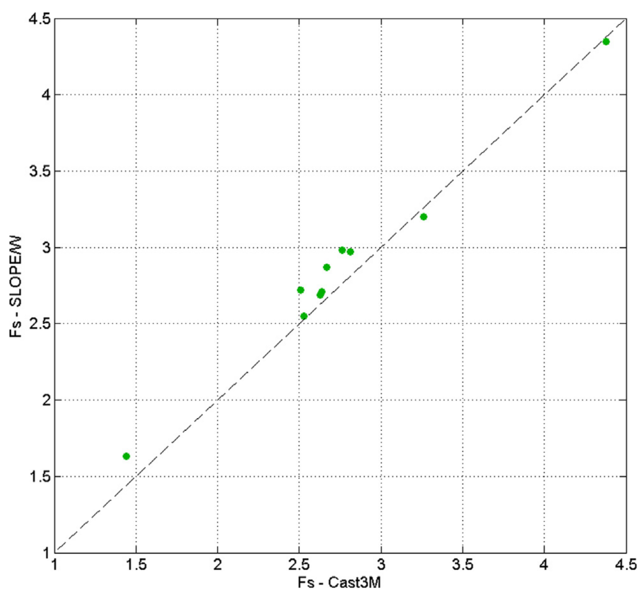

Fig. 5. Validation of the deterministic analysis.

represent the spatial variability of dry density in the three zones composing the dam section.

Autocorrelation lengths for dry density detailed in Table 5 show that considerable homogeneity is found in the UPS, whereas, with shorter autocorrelation lengths, the COR and DOS zones are more spatially variable. This difference can be explained by better selection of the material composing the upstream zone and greater attention given to its construction.

Table 5 also shows that the main spatial variability is in the vertical direction in which autocorrelation lengths are lower. This is due to the construction principle which is done by layers. Plots given in appendix show as information the measured values of the dry density (and the associated values of friction angle) against the elevation Z.

The nugget effect corresponds to about half the variance for the upstream shoulder (UPS) and to a slightly lower fraction for the downstream shoulder (DOS) and the core (COR). The nugget effect can be attributed to the mixture of the materials during their excavation from the borrow pits. In our case, it is considered as a microstructure whose scale is less than the sampling step.

3.3.3. Random field of shear strength parameters

The random field of dry density is obtained directly with the geostatistical analysis presented in last subsection. However, random fields of shear strength parameters cannot be obtained this way. In the approach implemented, physical relationships between geotechnical parameters are used to link the shear strength parameters to dry density. These relationships are listed in [42,43]. For the friction angle, Caquot's relation, described in Eq. (7), is used in the case of the dam studied to obtain the representation of the spatial variability of the friction angle through a random field of dry density. The k values used in Eq. (7) are respectively equal to 0.25, 0.32 and 0.22 for UPS, COR and DOS. These values are obtained in using Eq. (7) on each zone with the corresponding means of the friction angle (listed in Table 4) and means of the dry density (listed in Table 5). Fig. 8 shows an example of a realization of the random field of the friction angle. In the developed FE model, the autocorrelated points of the random fields correspond to the centroid of each element constituting the mesh.

The sensitivity analysis (Fig. 6) shows the interest of modeling cohesion as a random field. However, no relation exits between dry density and the effective cohesion of a soil, although a correlation can be found in undrained condition [30]. In the case of the dam studied, it was not possible to generate a random field of cohesion from the available data. This parameter is represented as a random variable in the probabilistic model.

3.3.4. Monte Carlo simulation results

MCS are used to assess the variability of the FoS by performing a large series of runs of the deterministic FE model by considering the probabilistic representation of the parameters of interest presented before. MCS are implemented by coupling the FE code Cast3M with the open-source reliability software OpenTURNS.

Three different probabilistic configurations are considered in the probabilistic analysis (Table 6):

- Configuration no. 1: LEM (Spencer method with search for circular slip surfaces) and random variable modeling with the commercial

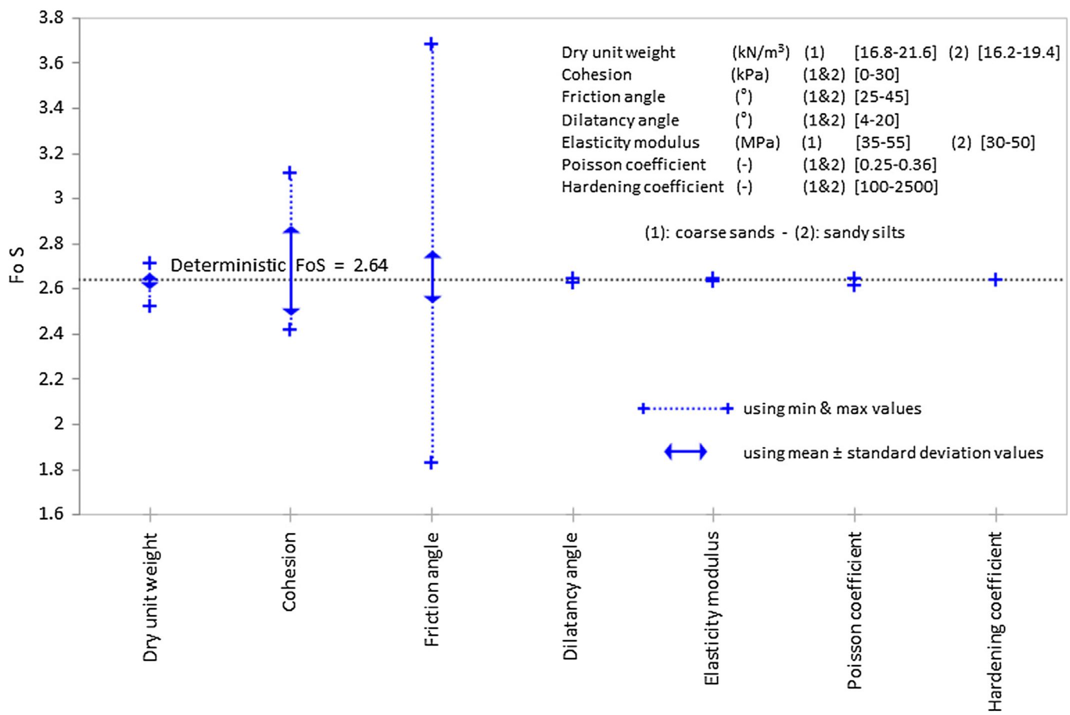

Fig. 6. Sensitivity analysis results.

Table 4
Probabilistic values of input parameters.

Soil type*	Parameter	Mean	Standard deviation	CoV (%)	Min	Max
UPS/DOS	Dry unit weight γ (kN m^{-3})	19.8	0.5	3	16.8	21.6
	Friction angle φ' (°)	34.8	1.3	4	25	45
	Cohesion c' (kPa)	8.9	8.1	91	0	30
COR	Dry unit weight γ (kN m^{-3})	17.9	0.6	3	16.2	19.4
	Friction angle φ' (°)	34.1	0.8	2	25	45
	Cohesion c' (kPa)	13.4	4.9	36	0	30

* UPS/DOS: Coarse sands (shoulders material); COR: Sandy silt (core material).

Table 5
Results of the geostatistical analysis of compaction control measurements (dry density).

ρ_d (t/m^3)	Mean	Variance	Nugget effect	Correlation length X	Correlation length Z
UPS	2.00	3.5×10^{-3}	1.6×10^{-3}	78.1 m	7.8 m
COR	1.83	3.6×10^{-3}	8.6×10^{-4}	13.0 m	1.5 m
DOS	2.05	2.8×10^{-3}	1.0×10^{-3}	4.9 m	1.9 m

software SLOPE/W;
- Configuration no. 2: FEM and random variable modeling with the FE code Cast3M;
- Configuration no. 3: FEM and random field modeling (for dry density and friction angle) with the FE code Cast3M.

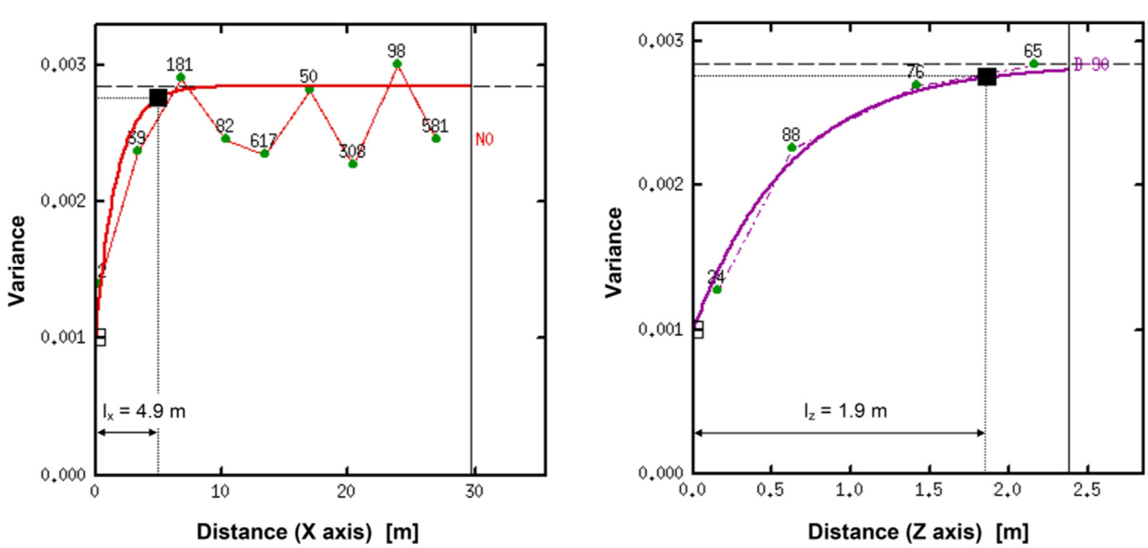

Fig. 7. Experimental variograms of dry density in the horizontal (left) and vertical (right) directions for the downstream shoulder (DOS).

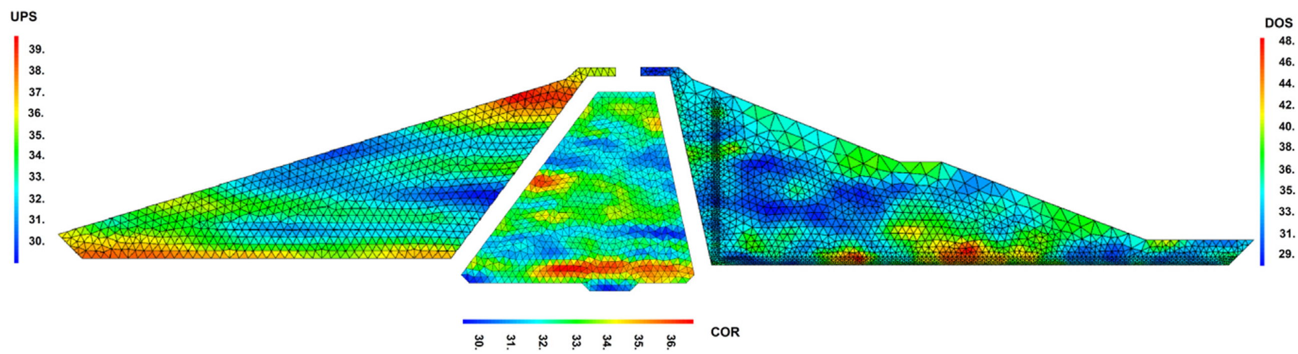

Fig. 8. Example of a realization of the random field of the friction angle (°).

Table 6
Calculation configurations for probabilistic analysis.

	Configuration no. 1	Configuration no. 2	Configuration no. 3
Software	SLOPE/W	Cast3M	Cast3M
Numerical method	LEM	FEM	FEM
Uncertain parameters			
Dry unit weight γ_d	Random variable	Random variable	Random field
Friction angle φ'	Random variable	Random variable	Random field
Cohesion c'	Random variable	Random variable	Random variable

The objectives are: (i) to compare increasingly complex approaches (Configuration no. 1 to Configuration no. 3) and (ii) to compare more particularly the use of random variables and random fields with FEM (Configuration no. 2 vs. Configuration no. 3).

100.000 simulations were performed for Configuration no. 1, while 10,000 were performed for the two others because FEM demands more computational effort. However, this number of simulations is sufficient to obtain accurate statistical responses, as seen in Fig. 9(a and b) showing the convergence of the mean and standard deviation of FoS. For each MC simulation involving FE analysis with random fields, the spatially autocorrelated soil property values are generated and assigned to each finite element constituting the mesh. Each simulation of a random field thus comprises a number of spatially autocorrelated values equal to the number of finite elements of the model. The mean values of FoS are equal to 2.75, 2.65 and 2.71 respectively for the three configurations, with the corresponding standard deviations equal to 0.17, 0.27 and 0.21. The probabilistic responses for each configuration are finally described in Fig. 10. The center of the box represents the second quartile Q2 of the sample whereas the box itself symbolizes the interquartile range (IQR), being equal to the difference between the 75th and 25th percentiles (resp. Q3 and Q1). The left and right whiskers represent the range between Q1 − 1.5 IQR and Q3 + 1.5 IQR and the points are outliers that fall outside this range.

Regarding the reliability index, Eq. (6) gives reliability indexes for the three configurations equal to 10.3, 6.1 and 8.1, respectively.

4. Discussion

4.1. Discussion on the stochastic finite element approach implemented

The aim of this article is to perform a probabilistic stability analysis for an existing earthfill dam using a Stochastic Finite Element Method and considering the spatial variability of soil properties based on field data (obtained from measurements made during the construction of the dam). Indeed, although other research works have dealt with the issue of probabilistic slope stability analysis, they generally consider arbitrary probabilistic distributions to model the uncertainties on soil properties.

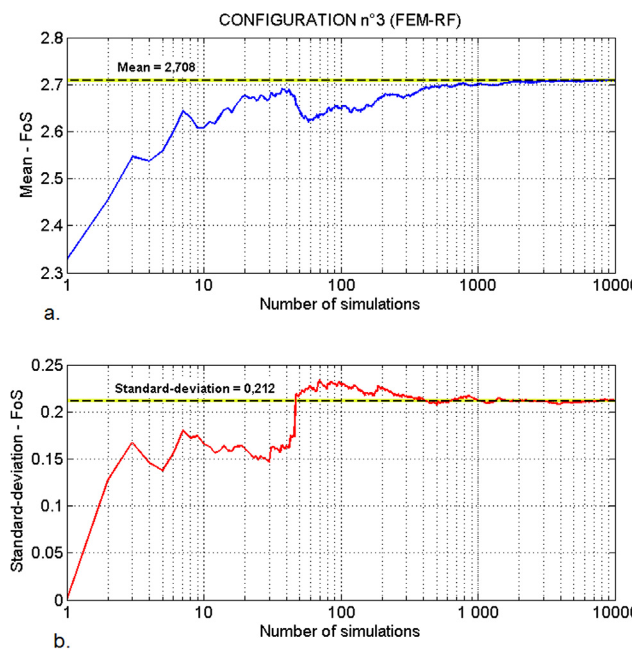

Fig. 9. Convergence of statistical moments (mean and standard deviation) of FoS. (a) Mean vs. number of runs. (b) Standard deviation vs. numbers of runs.

When spatial variability is considered through random fields, these random fields are seldom determined from real data. This article shows a probabilistic stability analysis for the case study of an existing earthfill dam using precisely located compaction control data. This geolocalization and the numerous available data allow the use of geostatistics to directly represent the spatial variability of parameters such as dry density. However, the spatial variability of other soil properties could be investigated as a function of the dataset available, as in Smith and Konrad [32] who considered the fines content of soil.

This article is focused on the uncertainty related to inherent soil spatial variability because it is the most significant source of geotechnical uncertainties, as mentioned in the introduction. Considering that empirical and theoretical relationships are used in this article, it could be interesting to consider the uncertainty of transformation in future works and the measurement error on the available data. Indeed, these two sources of uncertainty are known to be very difficult to quantify, although Phoon and Kulhawy [5,6] have proposed guidelines to overcome this problem.

In the procedure used on the case study, several hypotheses could have an influence on the results. For example, the choice of the ACF can affect the autocorrelation lengths and therefore the simulation of the random fields of the parameters. For the variograms plotted in Fig. 7, if gaussian or spherical models are chosen as ACF instead of the exponential model, the vertical and horizontal autocorrelation lengths will respectively be equal to l_x = 6.7 m or 4.7 m and l_z = 1.6 m or 1.2 m

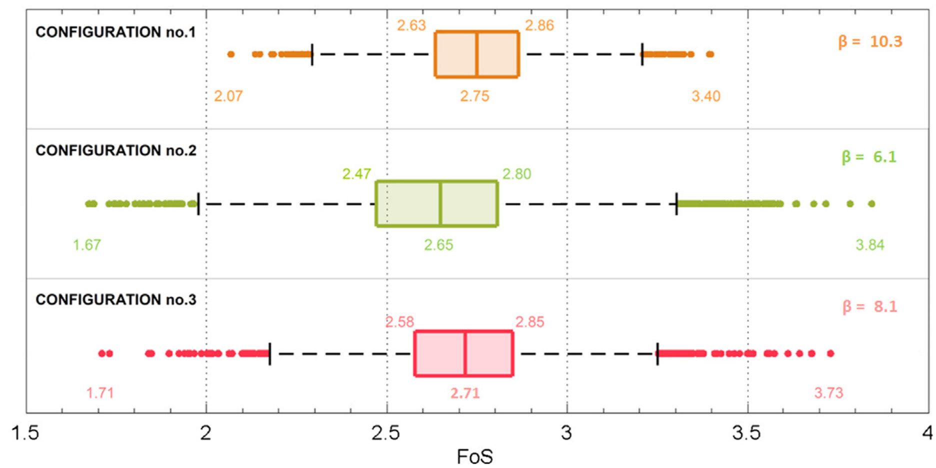

Fig. 10. Results and reliability indexes computed for the three configurations.

instead to $l_x = 4.9$ m and $l_z = 1.9$ m in the exponential case. These differences could have an influence on the computed FoS. Another example could be cited with the hypothesis on the terms k in Eq. (7). In this case study these parameters are estimated with the means of dry density and friction angle for the three zones of the studied dam, but another way could be used to obtain these values which are directly involved in the random field generation. Further investigations are necessary to quantify the influence of these hypotheses.

The question of SFEM and reliability methods can also been discussed. Direct MCS are performed in this case because they constitute a non-biased method and they are the easiest means to obtain a representative sample for assessing the variability of FoS. However, obtaining converged results in terms of mean and standard deviation requires performing a large number of simulations – 10 000 in the cases presented – which involve considerable computational efforts. For a more accurate assessment of the reliability index β or of the failure probability P_f, more calculations are necessary (generally, for an expected failure probability of $P_f = 10^{-n}$, 10^{n+2} simulations are needed), which it is not operational in this case. Thus, other reliability methods could be employed to quickly obtain the reliability index β or the failure probability P_f, like FORM/SORM, enhanced Monte-Carlo methods (Directional Simulations, Importance or Conditional Samplings), and the response surface, as described in [30].

4.2. Discussion on the results

4.2.1. Comparison of variability of FoS for the different configurations

The mean values of FoS obtained in the three configurations analyzed are close to the deterministic values obtained with the LEM model (i.e. 2.71) and the FEM model (i.e. 2.64). The distributions of FoS differ however concerning their scattering, as can be seen in Fig. 10. The computed FoS obtained in Configuration no. 1 is less scattered with a standard deviation of 0.17, while the standard deviations are 0.27 and 0.21 for Configurations no. 2 and no. 3, respectively. This may be due to the predefinition of the potential slip surfaces zone for the LEM model in Configuration no. 1 (limited to circular and relatively deep surfaces), whereas the FEM analysis can also lead to more superficial and/or not necessarily circular sliding surfaces.

The reliability indexes computed for all the configurations are very high, which means that the failure probability is close to zero. This illustrates the good design of the dam for the situation analyzed (i.e. normal operating level) which is generally not a risky situation. Lower reliability indexes will be found when analyzing trickier situations like earthquakes or the rapid drawdown of the dam reservoir. The normal operating level situation was chosen here because it remains that most representative of the structure's lifecycle and also because modeling this situation constitutes the base for all the others.

4.2.2. Comparison of random variables vs. random fields probabilistic approaches

When comparing configurations 2 and 3 it can be seen that taking spatial variability into account tends to reduce the main scattering of the samples. IQR is indeed larger in Configuration no. 2 [2.47–2.80] than in Configuration no. 3 [2.58–2.85]. This could be partly explained from the friction angle which is modeled as a random variable and as a random field in Configurations no. 2 and no. 3 respectively. Indeed, the mean of the friction angle is globally identical along the sliding surface from one simulation to another in Configuration no. 3, while the difference could be larger in the case of Configuration no. 2.

The mean values are also different between the two configurations. This could be explained by the fact that the effective friction angle is not modeled in the same way: on the one hand this parameter is modeled on the basis of triaxial tests; on the other hand it relies on measured dry density values. However, spatial variability modeling is in this specific case has a beneficial impact on the probabilistic response as it reduces the IQR and gives a higher reliability index than in random variable modeling. This is due to the averaging effect inherent to the random field representation: a low value of a parameter (e.g. of a friction angle) will not only have an impact on the FoS because this value is isolated and surrounded by other values that could be greater. Hence, in the case of the dam studied, modeling spatial variability with random fields is more representative of the physical reality and has a positive influence on dam reliability. The differences in the results obtained for configurations no. 2 and no. 3 remain overall low in terms of mean and standard deviation of the FoS. As the values obtained are high for the mean FoS and low for the standard deviation, the differences appear significant in terms of reliability index.

5. Conclusions

In this article, a stochastic finite element procedure based on project-specific data was implemented to assess the slope stability analysis of a case study of an earth dam. This procedure involved an evaluation of the input parameters required in an SFEM model based on field data. Furthermore, this evaluation was probabilistic concerning parameters that have a strong influence on the FoS. This paper performs a probabilistic stability analysis by SFEM for an existing earthfill dam, considering the spatial variability of soil properties based on field data. Indeed, the localization of the compaction control measurements performed during the earth dams' construction is put to good use in this approach thanks to the geostatistical analysis that allows modeling the spatial variability of soil properties by random fields. Finally, MCS were performed on the deterministic FEM model to give a probabilistic distribution of FoS, and thus a reliability evaluation from the reliability index. Such an approach could be used as part of a global dam safety assessment combined with a risk analysis like that described in [45].

Based on the results obtained on the case study, the following conclusions and statements can be presented:

(1) The probabilistic analysis performed in this article can be easily applied to limited datasets generally available for earth dams. It allows overcoming the small number of in-situ or laboratory geotechnical tests by taking advantage of available data.
(2) Geostatistics provide a powerful tool for assessing the spatial variability of soil properties, even in the particular case of embankment dams. It is interesting to take this variability into account because of its significant influence on FoS (and thus on the reliability index) as it tends to reduce failure probability. The use of geostatistical methods nonetheless requires a large sample of geolocalized data, as with the compaction control measurements in the case study. Nowadays, this geolocalization can be performed easily with GPS technology. However, geostatistical analysis is in most cases only possible on compaction control measurements, as in the case studied with dry density.
(3) The use of empirical and theoretical relationships between geotechnical properties is a simple way to obtain random fields of geotechnical soil properties other than dry density (permeability, friction angle, undrained cohesion). However, it is impossible in the case of effective cohesion because no physical relation exists with dry density. The use of relationships gives rise to another issue which is the implementation of measurement and/or transformation uncertainties in the model. This issue is not dealt with in the article and could be the subject of future research works.
(4) Comparing three configurations opposing increasingly complex approaches on the one hand, and random variables and random fields on the other, showed that, in the example of the dam studied, FEM gives a more scattered distribution than LEM but incorporates a better representation of the sliding mechanism. Modeling spatial variability is also beneficial as it gives a better representation of physical reality and has a positive impact on dam reliability.

This study also highlighted some possible improvements:

(1) For the sake of simplicity and consistency with other studies, only stationary Gaussian random fields were considered in this article. The effects of more complex random fields (non-stationary or non-Gaussian) could be investigated in specific studies. Indeed, earth dams are generally constructed with materials taken from several borrow pits, leading to potential heterogeneity of the fill.
(2) This article presented a 2D FE analysis including input parameters modeled by 2D random fields. The spatial variability of material properties as well as the mechanical stability to sliding can be further investigated by 3D analyses, which would better reflect that the material properties may vary differently in the space and that the sliding mechanism concerns more globally a volume.
(3) In this specific case of dam, very high reliability indexes, corresponding to a very low failure probability, were obtained. This was mainly due to the situation considered (i.e. normal operating level). Other situations could be considered to assess slope stability with such a probabilistic procedure, like earthquakes, rapid drawdowns, and floods. The reliability method used should be adapted to the situation studied according to the probabilistic output desired in order to optimize computational efforts.

Acknowledgement

The authors are grateful to the Compagnie d'Aménagement des Coteaux de Gascogne (CAGC) for its permission to use their data in this article. We also thank IRSTEA and Clermont-Auvergne University for funding this study.

Appendix

Figs. 11 and 12below show the measured values of the dry density (and the associated values of friction angle) against the elevation Z.

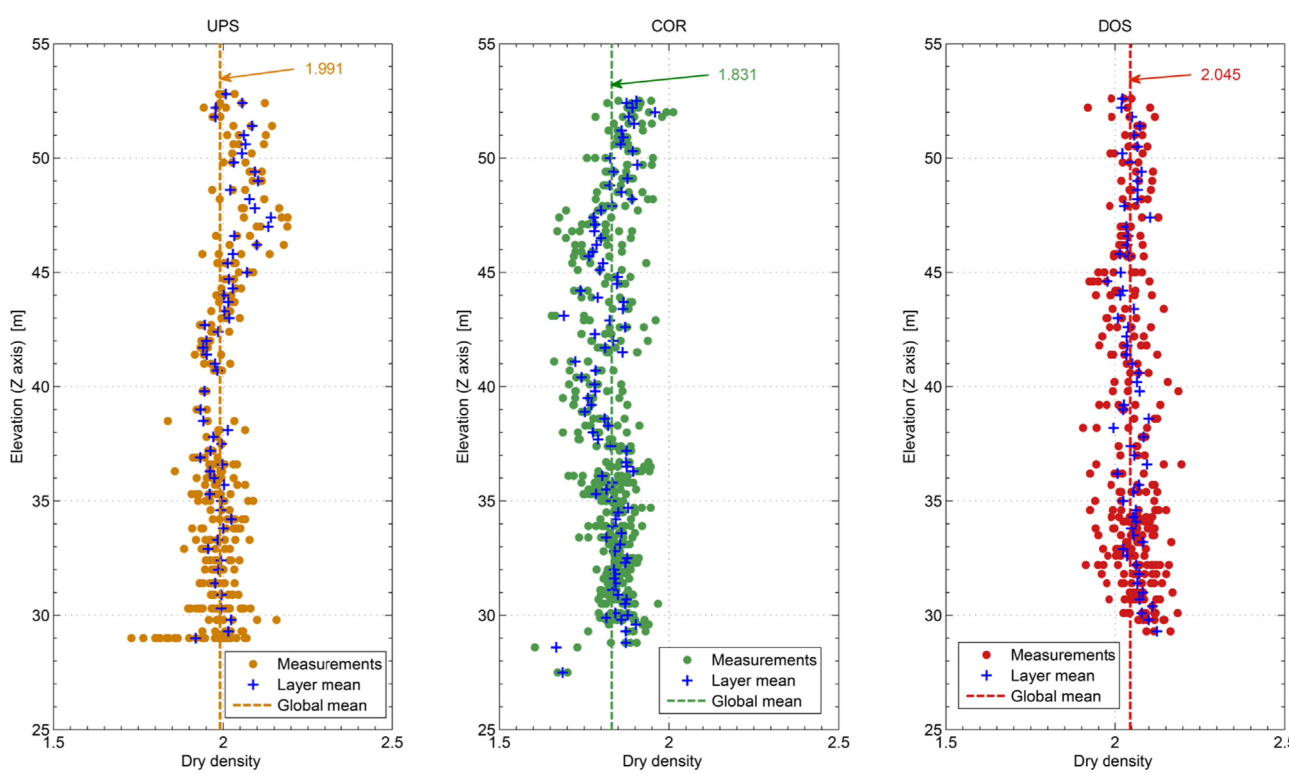

Fig. 11. Measured values of the dry density against the elevation Z.

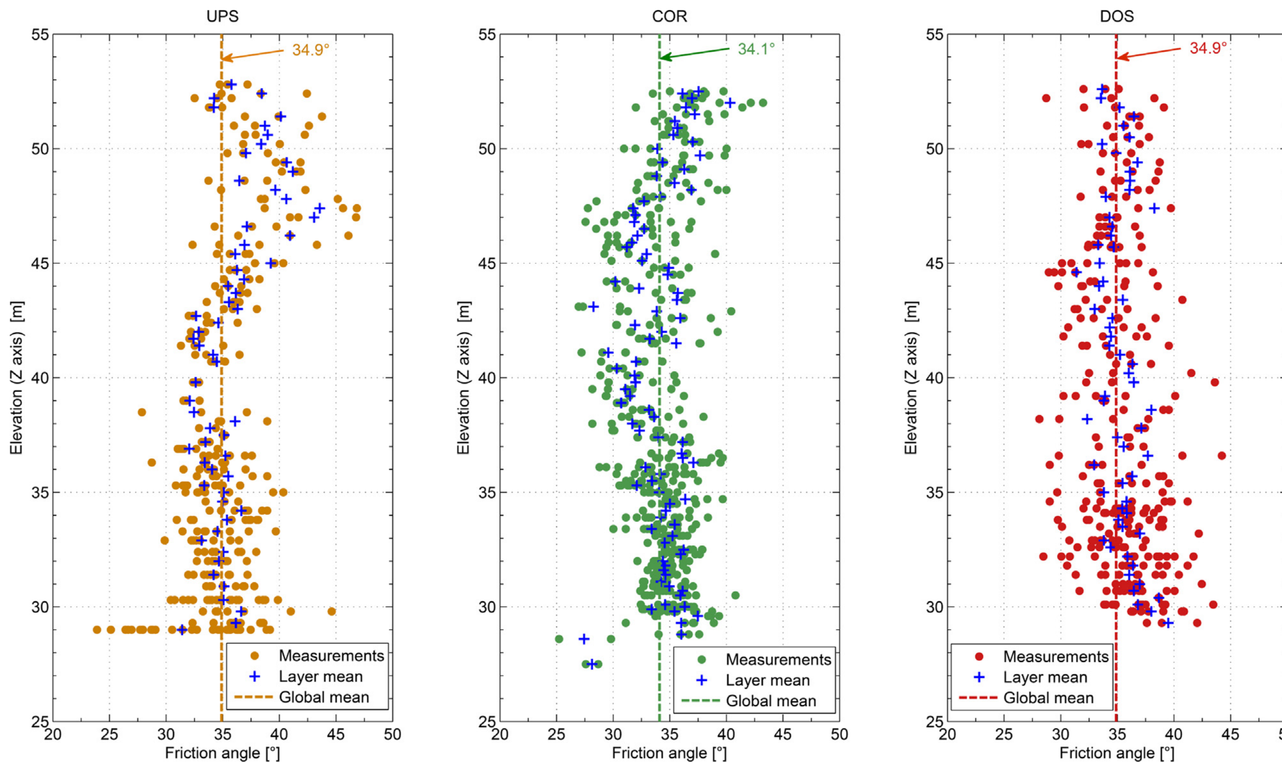

Fig. 12. Results of friction angle against the elevation Z.

References

[1] Christakos G. Modern statistical analysis and optimal estimation of geotechnical data. Eng Geol 1985;22(2):175–200.
[2] Suchomel R, Maši D. Comparison of different probabilistic methods for predicting stability of a slope in spatially variable c–φ soil. Comput Geotech 2010;37(1):132–40.
[3] Liu LL, Cheng YM, Zhang SH. Conditional random field reliability analysis of a cohesion-frictional slope. Comput Geotech 2017;82:173–86.
[4] Christian JT, Ladd CC, Baecher GB. Reliability applied to slope stability analysis. J Geotech Eng 1994;120(12):2180–207.
[5] Phoon KK, Kulhawy FH. Characterization of geotechnical variability. Can Geotech J 1999;36(4):612–24.
[6] Phoon KK, Kulhawy FH. Evaluation of geotechnical property variability. Can Geotech J 1999;36(4):625–39.
[7] Vanmarcke EH. Reliability of earth slopes. J Geotech Eng Divis 1977;103(11):1247–65.
[8] Fenton GA, Griffiths DV. Statistics of free surface flow through stochastic earth dam. J Geotech Eng 1996;122(6):427–36.
[9] Fenton GA, Griffiths DV. Extreme hydraulic gradient statistics in stochastic earth dam. J Geotech Geoenviron Eng 1997;123(11):995–1000.
[10] Griffiths DV, Fenton GA. Probabilistic analysis of exit gradients due to steady seepage. J Geotech Geoenviron Eng 1998;124(9):789–97.
[11] Cho SE. Effects of spatial variability of soil properties on slope stability. Eng Geol 2007;92(3):97–109.
[12] Srivastava A, Babu GLS, Haldar S. Influence of spatial variability of permeability property on steady state seepage flow and slope stability analysis. Eng Geol 2010;110(3–4):93–101. http://dx.doi.org/10.1016/j.enggeo.2009.11.006.
[13] Cho SE. Probabilistic assessment of slope stability that considers the spatial variability of soil properties. J Geotech Geoenviron Eng 2010;136(7):975–84.
[14] Jiang SH, Li DQ, Zhang LM, Zhou CB. Slope reliability analysis considering spatially variable shear strength parameters using a non-intrusive stochastic finite element method. Eng Geol 2014;168:120–8.
[15] Li DQ, Jiang SH, Cao ZJ, Zhou W, Zhou CB, Zhang LM. A multiple response-surface method for slope reliability analysis considering spatial variability of soil properties. Eng Geol 2015;187:60–72.
[16] Liu LL, Cheng YM, Jiang SH, Zhang SH, Wang XM, Wu ZH. Effects of spatial autocorrelation structure of permeability on seepage through an embankment on a soil foundation. Comput Geotech 2017;87:62–75.
[17] Vanmarcke EH. Random Fields: Analysis and Synthesis. Cambridge, MA: MIT Press; 1983.
[18] Gaouar M, Fogli M, Bacconnet C. Reliability of earth dams: an approach based on random fields models. In: International conference on applications of statistics and probabilities in civil engineering, Sydney – Australia; 2000. pp. 355–61.
[19] Auvinet G, Gonzalez J. Three-dimensional reliability analysis of earth slopes. Comput Geotech 2000;26(3):247–61.
[20] Griffiths DV, Huang J, Fenton GA. Influence of spatial variability on slope reliability using 2-D random fields. J Geotech Geoenviron Eng 2009;135(10):1367–78.
[21] Duncan JM. State of the art: limit equilibrium and finite-element analysis of slopes. J Geotech Eng 1996;122(7):577–96.
[22] Zienkiewicz OC, Humpheson C, Lewis R. Associated and non-associated visco-plasticity in soils mechanics. Geotechnique 1975;25(5):671–89.
[23] Matsui T, San KC. Finite element slope stability analysis by shear strength reduction technique. Soils Found 1992;32(1):59–70.
[24] Griffiths DV, Lane P. Slope stability analysis by finite elements. Geotechnique 1999;49(3):387–403.
[25] Cheng YM, Lansivaara T, Wei WB. Two-dimensional slope stability analysis by limit equilibrium and strength reduction methods. Comput Geotech 2007;34(3):137–50.
[26] Huang M, Jia CQ. Strength reduction FEM in stability analysis of soil slopes subjected to transient unsaturated seepage. Comput Geotech 2009;36(1–2):93–101.
[27] Liang R, Nusier BO, Malkawi AH. A reliability based approach for evaluating the slope stability of embankment dams. Eng Geol 1999;54(3):271–85.
[28] Xu B, Low B. Probabilistic stability analyzes of embankments based on finite-element method. J Geotech Geoenviron Eng 2006;132(11):1444–54.
[29] Degoutte G. Small dams: Guidelines for design, construction and monitoring. Cemagref Editions; 2002. ISBN: 9782853625517.
[30] Mouyeaux A. Fiabilité des barrages en remblai au glissement par MEFS. Editions Universitaire Européennes; 2017.
[31] Favre JL, Bekkouche A. Analyzes statistiques et modèles probabilistes pour les barrages en terre - Etat actuel et perspectives. In: Colloque technique, Comité Français des Grands Barrage, Paris; 1988.
[32] Smith M, Konrad JM. Assessing hydraulic conductivities of a compacted dam core using geostatistical analysis of construction control data. Can Geotech J 2011;48(9):1314–27. http://dx.doi.org/10.1139/t11-038.
[33] Carvajal C, Peyras L, Bacconnet C, Bécue JP. Probability modelling of shear strength parameters of RCC gravity dams for reliability analysis of structural safety. Eur J Environ Civ Eng 2009;13(1):91–119.
[34] Zheng H, Tham LG, Liu D. On two definitions of the factor of safety commonly used in the finite element slope stability analysis. Comput Geotech 2006;33(3):188–95.
[35] Abbo AJ, Sloan SW. A smooth hyperbolic approximation to the Mohr-Coulomb yield criterion. Comput Struct 1995;54(3):427–41.
[36] Mestat P. Lois de comportement des géomatériaux et modélisation par la méthode des éléments finis. In: Etudes et recherches des laboratoires des Ponts et Chaussées – Série Géotechnique (GT52); 1993.
[37] Griffiths DV, Fenton GA. Probabilistic slope stability analysis by finite elements. J Geotech Geoenviron Eng 2004;5:507–18.
[38] Huang J, Lyamin AV, Griffiths DV, Krabbenhoft K, Sloan SW. Quantitative risk assessment of landslide by limit analysis and random fields. Comput Geotech 2013;53:60–7.
[39] Gui S, Zhang R, Turner JP, Xue X. Probabilistic slope stability analysis with stochastic soil hydraulic conductivity. J Geotech Geoenviron Eng 2000;126(1):1–9.

[40] Bergado DT, Anderson LR. Stochastic analysis of pore pressure uncertainty for the probabilistic assessment of the safety of earth slopes. Soils Found 1985;25(2):87–105.
[41] Chowdhury RN, Xu DW. Geotechnical system reliability of slopes. Reliab Eng Syst Safe 1995;47(3):141–51.
[42] Kulhawy FH, Mayne PW. Manual on estimating soil properties for foundation design. Electric Power Research Inst., Palo Alto, CA (USA); Cornell Univ., Ithaca, NY (USA). Geotechnical Engineering Group; 1990.
[43] Monnet J. Les essais in situ en géotechnique. ISTE Editions; 2016.
[44] Carvajal C, Peyras L, Arnaud P, Boissier D, Royet P. Probabilistic modelling of flood water level for dam reservoirs. ASCE - J Hydrol Eng 2009;14(3):223–32.
[45] Peyras L, Carvajal C, Felix H, Bacconnet C, Royet P, Becue JP, et al. Probability-based assessment of dam safety using combined risk analysis and reliability methods – application to hazards studies. Eur J Environ Civ Eng 2012;16(7):795–817.
[46] Xiao T, Li D-Q, Cao Z-J, Au S-K, Phoon K-K. Three-dimensional slope reliability and risk assessment using auxiliary random finite element method. Comput Geotech 2016;79:146–58.
[47] Nishimura S-I, Shibata T, Shuku T. Diagnosis of earth-fill dams by synthesized approach of sounding and surface wave method. Georisk: Assess Manage Risk Eng Syst Geohazards 10.4: 312–9.
[48] Zheng D, Huang J, Li D-Q, Kelly R, Sloan S-W. Embankment prediction using testing data and monitored behavior: a Bayesian updating approach. Comput Geotech 2018;93:150–62.